Potential Energy Surface Reconstruction and Lifetime Determination of Molecular Double-Core-Hole States in the Hard X-Ray Regime

T. Marchenko, G. Goldsztejn, K. Jänkälä, O. Travnikova, L. Journel, R. Guillemin, N. Sisourat, D. Céolin, M. Žitnik, M. Kavčič, et al.

HAL Id: hal-01628469

https://hal.sorbonne-universite.fr/hal-01628469v1

Submitted on 3 Nov 2017

Potential energy surface reconstruction and lifetime determination of molecular double-core-hole states in hard x-ray regime.

T. Marchenko,[1, 2, *] G. Goldsztejn,[1, 3] K. Jänkälä,[4] O. Travnikova,[1, 2] L. Journel,[1, 2] R. Guillemin,[1, 2]

N. Sisourat,[1] D. Céolin,[2] M. Žitnik,[5] M. Kavčič,[5] K. Bučar,[5] A. Mihelič,[5] B. Cunha de Miranda,[1]

I. Ismail,[1] A. F. Lago,[6] F. Gel'mukhanov,[7, 8] R. Püttner,[9] M. N. Piancastelli,[1, 10] and M. Simon[1, 2]

[1]*Sorbonne Universités, UPMC Univ Paris 06, CNRS, UMR 7614,*
Laboratoire de Chimie Physique-Matière et Rayonnement, F-75005, Paris, France
[2]*Synchrotron SOLEIL, l'Orme des Merisiers, Saint-Aubin, BP 48, F-91192 Gif-sur-Yvette Cedex, France*
[3]*Max-Born-Institut, Max-Born-Straße 2A, 12489 Berlin, Germany*
[4]*Nano and Molecular Systems Research Unit, University of Oulu, P.O. Box 3000, 90014 Oulu, Finland*
[5]*Jožef Stefan Institute, SI-1001 Ljubljana, Slovenia*
[6]*Centro de Ciências Naturais e Humanas, Universidade Federal do ABC (UFABC), 09210-580, Santo André, SP, Brazil*
[7]*Theoretical Chemistry & Biology, School of Biotechnology,*
Royal Institute of Technology, SE-106 91 Stockholm, Sweden
[8]*Institute of Nanotechnology, Spectroscopy and Quantum Chemistry,*
Siberian Federal University, 660041 Krasnoyarsk, Russia
[9]*Fachbereich Physik, Freie Universität Berlin, D-14195 Berlin, Germany*
[10]*Department of Physics and Astronomy, Uppsala University, PO Box 516, SE-751 20 Uppsala, Sweden*
(Dated: September 1, 2017)

A combination of resonant inelastic x-ray scattering and resonant Auger spectroscopy provides complementary information on the dynamic response of resonantly excited molecules. This is exemplified for CH_3I, for which we reconstruct the potential energy surface of the dissociative I $3d^{-2}$ double-core-hole state and determine its lifetime. The proposed method holds a strong potential for monitoring the hard x-ray induced electron and nuclear dynamic response of core-excited molecules containing heavy elements, where *ab initio* calculations of potential energy surfaces and lifetimes remain challenging.

Hard x-ray radiation, with photon energy above 1 keV, can excite deep core shells of heavy atoms (Cl $1s$, S $1s$, I $2p$ etc) and may cause breakage of the chemical bonds and drastic changes to the electronic structure. The interplay between the induced nuclear and electron dynamics determines the response of a core-excited molecule. In the case of resonant excitation to a dissociative molecular state, the time evolution of the relaxation process is determined by the potential energy surface (PES) and the lifetime of the excited state. The so called "core-hole clock" spectroscopy (CHCS) allows probing ultrafast dynamics, occurring in a resonantly core-excited molecule within the core-hole lifetime, through control over the photon energy [1–4].

Resonant inelastic x-ray scattering (RIXS) and resonant Auger electron spectroscopy (RAS) are the two CHCS techniques relevant, respectively, to the measurements of x-ray photons or Auger electrons emitted in the course of relaxation of core-excited molecular states. As the probability of radiative relaxation of core-excited atoms increases with atomic number, both RIXS and RAS become equally relevant in the hard x-ray regime [5–14]. However, the major difference between these techniques appears in the electronic final states reached upon relaxation. In the case of RIXS, the molecule remains neutral with an electron in the excited orbital and a single hole, whereas in the case of resonant spectator Auger decay, the molecule becomes singly charged with an electron in the excited orbital and a double hole.

Spectroscopy of double core-hole (DCH) states, created either with intense XFEL radiation through multiphoton absorption [15–17] or with high-energy photons provided by synchrotron radiation [18–23], has been a hot topic in the recent years. The quantitative understanding of hard x-ray induced processes in polyatomic molecules [24], including nuclear dynamics of DCH states in molecules, formed in the course of cascade relaxations, is of particular interest in relation to radiation-induced damage in organic tissue and coherent diffraction imaging [25, 26].

In this Letter, we demonstrate an original method to extract information on the electron and nuclear dynamic response of molecules in DCH states, created with hard x-ray radiation. In contrast to soft x-ray region, where nuclear dynamics occurs in a core-excited state, a short lifetime of a core-excited state in the hard x-ray regime allows a simple and, hence, robust way to reconstruct the PES that affects the evolution of a nuclear wave packet (WP) in the final state. Furthermore, we obtain an estimate of the I $3d^{-2}$ DCH state lifetime, which determines the dynamics of the electronic structure evolution at the subsequent relaxation step. Our experimental method is validated by comparing the results obtained for CH_3Cl molecule with *ab initio* calculations of PES and the value of the Cl $2p^{-2}$ DCH lifetime estimated with other experimental methods. The advantage of our approach is especially significant in molecules, such as CH_3I, that contain heavy multielectron atoms and, thus, present a serious

challenge for *ab initio* description due to a large number of shells and the necessity to account for the electronic relaxation effects.

The RIXS measurements were performed at the ID26 beamline at the European Synchrotron Radiation Facility (ESRF). The experimental setup and the experimental settings are described in detail in [12, 27]. The RIXS spectra corresponding to the $L_3M_{4,5}$ transition were acquired with a total instrumental resolution of ≈ 0.65 eV determined from the width of the elastic peak, which includes the incident photon bandwidth and the spectrometer resolution.

The RAS measurements were performed at the endstation HAXPES, based on a hemispherical electron analyzer installed on the GALAXIES beamline at the synchrotron SOLEIL [28, 29]. The spectrometer is set parallel to the light polarization vector. The $L_3M_{4,5}M_{4,5}$ Auger spectra were recorded with the total resolution of ≈ 0.6 eV, which includes the photon bandwidth, the spectrometer resolution and the thermal Doppler broadening.

The RIXS and RAS measurements are presented in Figure 1 in the form of 2D maps, obtained by recording the spectra while changing the incident photon energy with a step of 0.2 eV around the I L_3 edge. Below the ionization threshold located around 4565 eV, both maps contain resonant lines dispersing with photon energy. The resonant excitation from the I $2p_{3/2}$ shell to the lowest unoccupied molecular orbital (LUMO) $15a_1$ occurs at 4559.2 eV photon energy. Above ionization threshold the maps display the onset of non-resonant $L_3M_{4,5}$ fluorescence and $L_3M_{4,5}M_{4,5}$ normal Auger lines independent of the photon energy. The rich multiplet Auger structure is assigned in the Supplemental Material [30]. For a further analysis, we select in both maps a well separated resonant line marked with a circle and trace its spectral shape as a function of photon energy around the $2p_{3/2} \to 15a_1$ resonant transition. The final state configuration for the selected lines is $3d_{5/2}^{-1}\text{LUMO}^*$ in the case of RIXS and $(3d_{5/2}^{-2})_4\text{LUMO}^*$ in the case of RAS. Figure 1(c) shows the full width at half maximum (FWHM) of the selected RIXS and Auger lines as a function of the incident photon energy around the LUMO absorption resonance. The error bars are extracted from the fit of the experimental spectra with Voigt profiles using the SPANCF macro package [31, 32].

The cross section for RIXS and RAS in the case of dissociative intermediate and final states is described by the generalized Kramers-Heisenberg formula [33]. In Franck-Condon and Born-Oppenheimer approximations the dipole and Coulomb transition matrix elements are independent of the nuclear coordinates and the expression for the cross section for a given final state simplifies
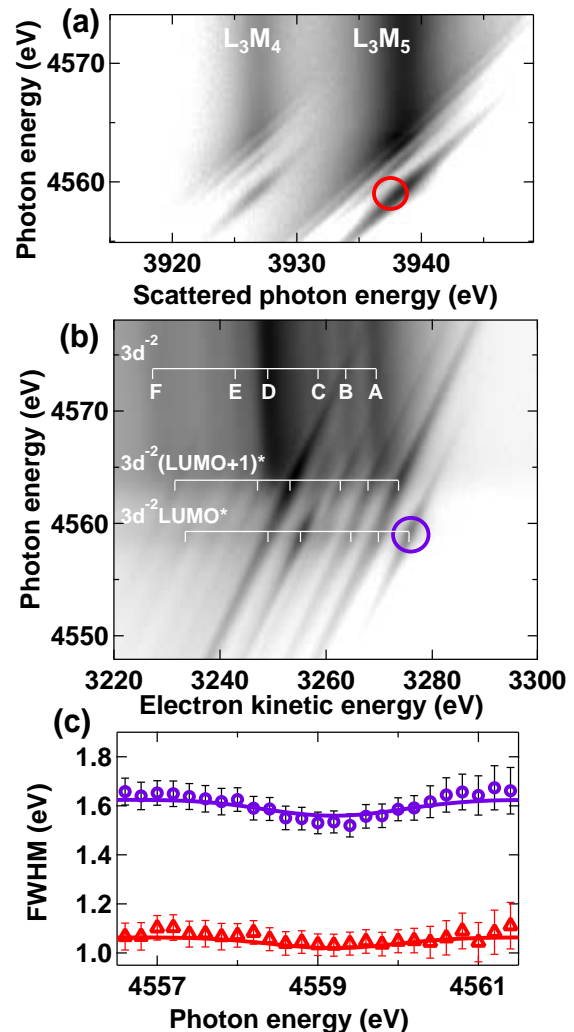

FIG. 1: (a) RIXS $L_3M_{4,5}$ and (b) Auger $L_3M_{4,5}M_{4,5}$ spectra recorded in CH_3I near the I L_3 edge. A detailed assignment of the labeled Auger lines is presented in the Supplemental Material. (c) FWHM of RIXS emission line (triangles) and Auger line (circles) selected in (a) and (b), respectively, as a function of photon energy around the LUMO resonance. Error bars are obtained from the fits of the experimental spectra. Solid lines show simulations based on Eqs.2 and 3.

to:

$$\sigma(\omega, \omega') \propto \int\limits_0^\infty dE_f \left| \sum_c \frac{\langle \chi_f | \chi_c \rangle \langle \chi_c | \chi_o \rangle}{\omega - \omega_{co} - \Delta E_c + \imath \Gamma_c} \right|^2$$
$$\times L(\omega - \omega' - \omega_{fo} - \Delta E_f, \Gamma_f) \tag{1}$$

Here the subscripts $i = f$, c and o stand respectively for the final, intermediate and ground molecular states, ω is the incident photon energy, ω' is the energy of the scattered photon or of the ejected Auger electron, $\omega_{jo} \equiv U_j(r_0) - \mathcal{E}_o$ is the energy of the $o \to j = c, f$ vertical transition, $\mathcal{E}_o$ is the total energy of the ground state

(electronic + nuclear), $\Gamma_{c,f}$ are the lifetime broadenings of the intermediate and final states described by the dissociative potentials $U_{c,f}(r)$, $\Delta E_{c,f} = E_{c,f} - \Delta U_{c,f}$ are the local nuclear kinetic energies at the point of the vertical transition $r = r_0$, $\Delta U_{c,f} \equiv U_{c,f}(r_0) - U_{c,f}(r \rightarrow \infty)$ and $E_{c,f}$ are the nuclear kinetic energies at $r \rightarrow \infty$. The numerator in Eq.(1) contains Franck-Condon (FC) overlaps between the nuclear wave functions χ_i and $L(\omega - \omega' - \omega_{fo} - \Delta E_f, \Gamma_f)$ is the normalized Lorentzian function with the FWHM equal to Γ_f that accounts for energy conservation throughout the whole absorption-decay process.

In our case both the core-excited and final states are dissociative along the C–I bond [12]. However, due to the large reduced mass and an extremely short lifetime of only 200 as of the I $2p_{3/2}^{-1}$ core-excited state [35], we can neglect the propagation of the nuclear WP in the intermediate state and consider an instantaneous transfer [4] of the initial WP $|\chi_o\rangle$ to the final state at the equilibrium internuclear distance r_0=2.139 Å. Consequently, the numerator in Eq.(1) describes a projection of the ground-state wave function localized near the equilibrium r_0 onto the continuum wave function in the final state $|\langle \chi_f | \chi_o \rangle|^2$. Furthermore, during fast scattering the nuclei have no time to change the local velocities as well as the local kinetic energies $\Delta E_c \approx \Delta E_f \equiv \epsilon$. Then the cross section reads

$$\sigma(\omega, \omega') \propto \int_{-\Delta U_f}^{\infty} d\epsilon \exp\left(-\frac{\epsilon^2}{\Delta_f^2}\right)$$
$$\times L(\omega - \omega_{co} - \epsilon, \Gamma_c) L(\omega - \omega' - \omega_{fo} - \epsilon, \Gamma_f), \quad (2)$$

where $\Delta_f = \mathcal{F}_{fo} a_o$ is the width of the FC distribution connecting the ground and the final states, $\mathcal{F}_{fo}$ is the absolute value of the gradient of the PES of the dissociative final state at the equilibrium internuclear distance, $a_o = \left(\frac{\hbar}{\mu \omega_o}\right)^{1/2}$ is the width of the nuclear WP in the ground state, μ is the reduced mass of the molecule with $\frac{1}{\mu} = \frac{1}{m_{CH_3}} + \frac{1}{m_I}$ and ω_o is the vibrational frequency along the C–I bond.

When the lifetime width of the final state is negligible $\Gamma_f \ll \Gamma_c, \Delta_f$, then $L(\omega - \omega' - \omega_{fo} - \epsilon, \Gamma_f) \approx \delta(\omega - \omega' - \omega_{fo} - \epsilon)$ and the cross section can be expressed analytically [34]:

$$\sigma(\omega, \omega') \propto \exp\left(-\frac{(\omega - \omega' - \omega_{fo})^2}{\Delta_f^2}\right)$$
$$\times L(\omega' - \omega_{co} + \omega_{fo}, \Gamma_c). \quad (3)$$

This approximation is generally valid in the case of RIXS [5, 8, 12]. However, in the case of RAS, the lifetime broadening of the DCH final state may be non-negligible and the cross section must be evaluated using Eq.(2).

Convolution of the theoretical cross sections in Eqs.(2) and (3) with a Gaussian describing instrumental func-

tion allows for a direct comparison with the experimental results presented in Fig.1(c). In our simulations we fixed the following parameters: ω_{co}=4559.2 eV, ω_{fo}=620.9 eV in the case of RIXS and ω_{fo}=1283.2 eV in the case of Auger as follows from the experimental observations, $\Gamma_c(2p_{3/2}^{-1})$=2.7 eV [35], reduced mass of CH$_3$I μ=13.4 amu, C–I vibrational frequency ω_o=16 THz, which gives $a_o = 0.07$ Å. The unknown values for the lifetime broadening of the DCH final state in the case of Auger $\Gamma_f(3d_{5/2}^{-2})$ and the gradients $\mathcal{F}_{fo}(3d_{5/2}^{-2})$ and $\mathcal{F}_{fo}(3d_{5/2}^{-1})$ of the PES of the final states at the equilibrium internuclear distance were kept as free parameters and have been determined from the fit exhibiting an excellent agreement with the experimental data.

The line narrowing at the resonant absorption energy of 4559.2 eV observed in both cases in Fig.1(c) is due to the quenching of the vibrational broadening reflected by the FC distribution in the core-excited state and was previously observed in molecular RIXS and RAS spectra [5, 9, 12]. The overall larger FWHM for the Auger line as compared to the RIXS line reflects two important differences between the final states. Close to the resonance, where the line width is mainly determined by the lifetime broadening, the FWHM of the Auger line indicates a larger lifetime broadening of the final $3d_{5/2}^{-2}$ DCH state with respect to the $3d_{5/2}^{-1}$ single core-hole (SCH) state. At the photon energies above or below the resonance, where the line width is strongly dependent on the FC dynamical broadening, the larger width of the Auger line indicates a larger width of the FC distribution Δ_f and, consequently, a more dissociative character of the $3d_{5/2}^{-2}$ DCH state as compared to the $3d_{5/2}^{-1}$ SCH state. In spite of the lack of ab $initio$ calculations that could reproduce these differences, we can elucidate and quantify the observed effect directly from our measurements.

Our results provide us with two important findings. First, the extracted value $\Gamma_f(3d_{5/2}^{-2}) = 1.05 \pm 0.05$ eV shows that the lifetime $\tau \propto 1/\Gamma$ of the DCH state is 0.6 fs that is around two times shorter than the lifetime of the SCH state τ=1.2 fs, where $\Gamma_f(3d_{5/2}^{-1}) = 0.56 \pm 0.05$ eV [35]. The lifetimes of $1s^{-2}$ DCH and the corresponding $1s^{-1}$ SCH states were previously reported for Ca, V, Cr, Co and Zn atoms [36], where the former were found to be 2.2 times shorter than the latter. In our recent work on $1s^{-2}$ DCH states in neon [23] and $2p^{-2}$ DCH states in argon [37] we have reported the ratios of 2.9 and 2.8, respectively. In order to validate our method, we have applied it to the previously measured RIXS and RAS in CH$_3$Cl excited at the Cl K-shell [9]. The extracted lifetime broadening of the Cl $2p^{-2}$ state $\Gamma(2p^{-2}) = 0.25 \pm 0.02$ eV that is around 2.9$\pm$0.2 times larger than $\Gamma(2p^{-1}) = 0.086$ eV [38], is consistent with the observations in argon [37]. The obtained value of the Cl $2p^{-2}$ lifetime broadening explains also the discrepancy between the experimental
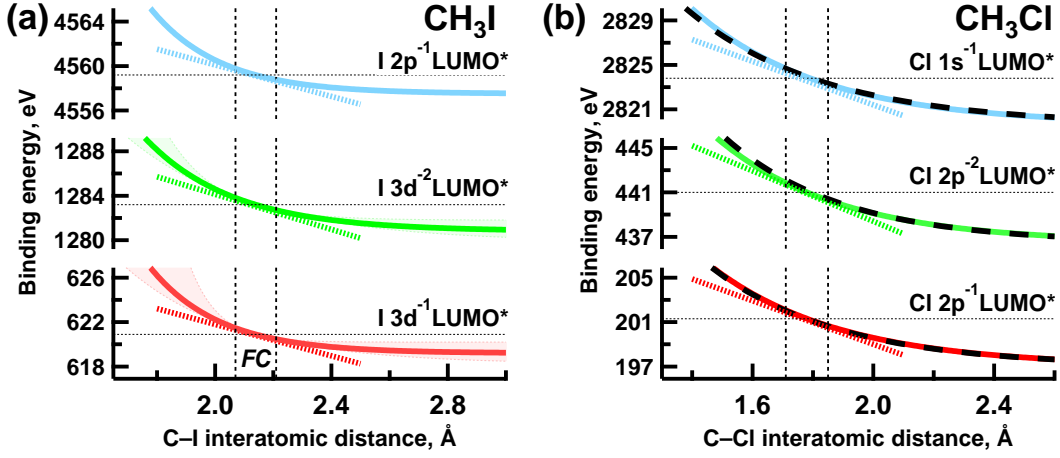
FIG. 2: PES reconstructed from the experimental data in (a) CH$_3$I and (b) CH$_3$Cl for the intermediate and final SCH and DCH states reached after RIXS or resonant Auger decay, respectively. The vertical lines mark the FC zone determined by the size a_o of the ground-state vibrational wave function. The shaded area in a) corresponds to the uncertainty of 1 eV for the asymptotic PES values calculated for atomic iodine. In CH$_3$Cl the reconstructed PES of the final states (solid lines) are compared to the results obtained with *ab initio* calculations (dashed lines).
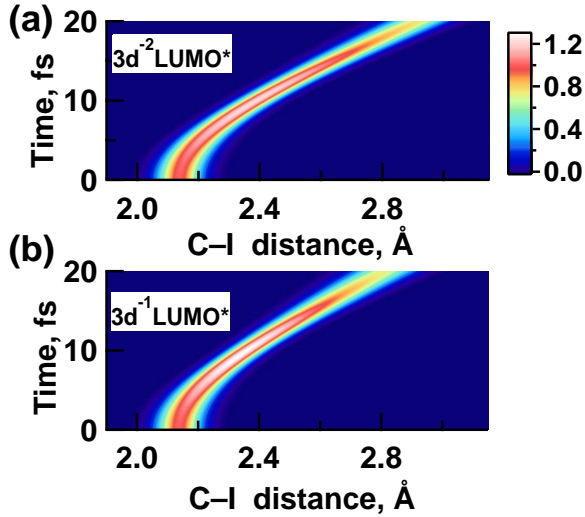

FIG. 3: Nuclear WP propagation along the simulated PES in (a) $3d_{5/2}^{-2}$LUMO* DCH and (b) $3d_{5/2}^{-1}$LUMO* SCH states.

data and simulations of the resonant Cl KLL Auger line using Eq.(3), where the lifetime of the final state was neglected [9]. As suggested in [23], the $\Gamma_{DCH}/\Gamma_{SCH}$ ratio must be dependent on the effective charge of the nucleus seen by electrons as well as on principal quantum number of the shells involved in the relaxation. For atoms with high atomic number and consequently, large effective charge, the ratio is expected to converge to 2. Our results are in line with this hypothesis and provide a test case for further theoretical modeling.

A second finding concerns the obtained absolute values

of the PES gradients at the equilibrium C–I interatomic distance: $\mathcal{F}_{fo}(3d_{5/2}^{-2}) = 7.9 \pm 0.3$ eV/Å, $\mathcal{F}_{fo}(3d_{5/2}^{-1}) = 7.1 \pm 0.3$ eV/Å. A dissociative potential $U_f(r)$ can be described by an exponential shape [39]:

$$U_f(r) = \Delta U_f \exp\left[\left(\frac{-\mathcal{F}_{fo}}{\Delta U_f}\right)(r - r_0)\right] + U_f(r \to \infty) \quad (4)$$

Here $U_f(r_0)$ is known from the experiment and the asymptotic PES value at large C–I distances, where dissociation is completed, $U_f(r \to \infty)$, can be calculated from the transition energies in atomic iodine and the molecular dissociation energy in the ground state. Atomic transition energies were calculated using relativistic Grasp2k code [40] in the single configuration scheme. Note that in the case of RIXS, where both the intermediate and the final states are dissociative SCH states, their PES can often be considered as parallel to each other [5, 12]. Therefore, we can assume the gradients of the I $2p_{3/2}^{-1}$LUMO* and $3d_{5/2}^{-1}$LUMO* states to be equal at r_0.

Fig. 2(a) shows the simulated PES of the intermediate $2p_{3/2}^{-1}$LUMO*, the final $3d_{5/2}^{-1}$LUMO* SCH and the final $3d_{5/2}^{-2}$LUMO* DCH states. This is an important outcome of our experimental analysis, since the existing theoretical tools for molecular PES calculations are so far not suitable for systems containing heavy multielectron elements. We confirm the reliability of our method using the case of CH$_3$Cl excited at the Cl K-shell [9] (Fig. 2(b)). The extracted absolute values of the PES gradients at the equilibrium C–Cl interatomic distance, $\mathcal{F}_{fo}(2p^{-2}) = 11.1 \pm 0.3$ eV/Å and $\mathcal{F}_{fo}(2p^{-1}) = 10 \pm 0.3$ eV/Å, provide a perfect agreement between the PES sim-

ulated with our method using Eq.(4) and the results of *ab initio* calculations using MOLPRO package [41] at the CASSCF level, where we chose a Gaussian basis set aug-cc-pCVTZ [42, 43], to take into account core-core and core-valence correlation effects, and included relativistic corrections with the use of the Douglas-Kroll Hamiltonian [44, 45].

The obtained PES allow predicting the dissociation dynamics in the final states. We have adopted a method that uses an analytic representation of the WP based on Heller's semiclassical approach and has proven to provide an excellent agreement with the numerical solution of the time-dependent Schrödinger equation [39, 46, 47]. Fig. 3(a) and (b) show the time evolution of the ordinary norm-conserving WP $|\chi(r,t)|^2$ in CH_3I along the simulated dissociative PES of the final $3d_{5/2}^{-2}$LUMO* DCH and $3d_{5/2}^{-1}$LUMO* SCH states, respectively. In both cases we can observe a narrowing of the WP width by 20-30% from its initial value occurring around t=10 fs and a subsequent broadening during further evolution. The observed narrowing effect occurs in CH_3I at times significantly exceeding the determined 0.6 fs lifetime of the DCH state, when the population of this state is considerably depleted due to the Auger decay. However, it may play a role in molecules with light atomic constituents such as hydrogen halides undergoing fast dissociation [14].

The predicted collapse of the WP width reflects the topology of the PES. A variation of PES gradient in the FC zone, determined by $d^2U_f(r_o)/dr^2 \propto \mathcal{F}_{fo}^2/\Delta U_f$, sets the initial conditions for the continuum vibrational wave functions composing a coherent nuclear WP in such a way that the tail of the WP propagates with a higher phase velocity than its front. In the course of propagation, the tail components of the WP may catch up and eventually overtake the front, which results in a spatial narrowing and a subsequent broadening of the WP width.

In conclusion, we have demonstrated a novel experimental method to obtain information on the lifetime and PES of dissociative SCH and DCH states in molecules, core-excited with hard x-ray radiation. Our approach provides a unique opportunity to determine the time scales for evolution of electronic and molecular structure in molecules containing heavy multielectron atoms, where *ab initio* description so far remains challenging. The method can be directly applied to other quasi-diatomic molecules where nuclear dynamics can be described with a dominant dissociative degree of freedom along the molecular axis. Generalization to polyatomic molecules with multiple dissociative degrees of freedom requires inclusion of multidimensional Franck-Condon factors in the adapted version of the Kramers-Heisenberg formula.

* E-mail:tatiana.marchenko@upmc.fr

[1] P. Morin and I. Nenner, Phys. Rev. Lett., **56**, 1913 (1986).

[2] O. Björneholm, S. Sundin, S. Svensson, R. R. T. Marinho, A. Naves de Brito, F. Gel'mukhanov, and H. Ågren, Phys. Rev. Lett., **79**, 3150 (1997).

[3] R. Feifel, F. Burmeister, P. Sałek, M. N. Piancastelli, M. Bässler, S. L. Sorensen, C. Miron, H. Wang, I. Hjelte, O. Björneholm *et al.*, Phys. Rev. Lett., **85**, 3133 (2000).

[4] F. Gel'mukhanov and H. Ågren, Phys. Rep. **312**, 87 (1999).

[5] M. Simon, L. Journel, R. Guillemin, W. C. Stolte, I. Minkov, F. Gel'mukhanov, P. Sałek, H. Ågren, S. Carniato, R. Taïeb *et al.*, Phys. Rev. A. **73**, 020706 (2006).

[6] L. Journel, L. El Khoury, T. Marin, R. Guillemin, S. Carniato, A. Avila, R. Delaunay, C. F. Hague, and M. Simon, Rev. Sci. Instrum. **80**, 93105 (2009).

[7] M. Kavčič, M. Žitnik, K. Bučar, A. Mihelič, S. Carniato, L. Journel, R. Guillemin, and M. Simon, Phys. Rev. Lett. **105**, 113004 (2010)

[8] R. Bohinc, M. Žitnik, K. Bučar, M. Kavčič, L. Journel, R. Guillemin, T. Marchenko, M. Simon, and W. Cao, J. Chem. Phys. **139**, 134302 (2013).

[9] M. N. Piancastelli, G. Goldsztejn, T. Marchenko, R. Guillemin, R. K. Kushawaha, L. Journel, S. Carniato, J.-P. Rueff, D. Céolin, and M. Simon, J. Phys. B **47**, 124031 (2014).

[10] G. Goldsztejn, T. Marchenko, D. Céolin, L. Journel, R. Guillemin, J.-P. Rueff, R. K. Kushawaha, R. Püttner, M. N. Piancastelli and M. Simon, Phys. Chem. Chem. Phys., **18**, 15133 (2016).

[11] O.Travnikova, T. Marchenko, G. Goldsztejn, K. Jänkälä, N. Sisourat, S. Carniato, R. Guillemin, L. Journel, D. Céolin, R. Püttner *et al.* Phys. Rev. Lett., **116**, 213001 (2016).

[12] T. Marchenko, L. Journel, T. Marin, R. Guillemin, S. Carniato, M. Žitnik, K. Bučar, M. Kavčič, A. Mihelič, J. Hoszowska *et al.*, J. Chem. Phys. **134**, 144308 (2011).

[13] T. Marchenko, S. Carniato, L. Journel, R. Guillemin, E. Kawerk, M. Žitnik, M. Kavčič, K. Bučar, R. Bohinc, M. Petric *et al.*, Phys. Rev. X **5**, 031021 (2015).

[14] O.Travnikova, N. Sisourat, T. Marchenko, G. Goldsztejn, R. Guillemin, L. Journel, D. Céolin, I. Ismail, A.F. Lago, R. Püttner *et al.* Phys. Rev. Lett., **118**, 213001 (2017).

[15] L. Young, E. P. Kanter, B. Krässig, Y. Li, A. M. March, S. T. Pratt, R. Santra, S. H. Southworth, N. Rohringer, L. F. DiMauro *et al.*, Nature, **466**, 56 (2010).

[16] N. Berrah, L. Fang, B. Murphy, T. Osipov, K. Ueda,

E. Kukk, R. Feifel, P. Van der Meulen, P. Salen, H. T. Schmidt *et al.*, Proceedings of the National Academy of Sciences, **108**,16912 (2011).

[17] P. Salén, P. Van der Meulen, H. T. Schmidt, R. D. Thomas, M. Larsson, R. Feifel, M. N. Piancastelli, L. Fang, B. Murphy, T. Osipov *et al.*, Phys. Rev. Lett., **108**, 153003 (2012).

[18] J. H. D. Eland, M. Tashiro, P. Linusson, M. Ehara, K. Ueda and R. Feifel, Phys. Rev. Lett., **105**, 213005 (2010).

[19] P. Lablanquie, F. Penent, J. Palaudoux, L. Andric, P. Selles, S. Carniato, K. Bučar,M. Žitnik, M. Huttula, J. H. D. Eland *et al.*, Phys. Rev. Lett., **106**, 063003 (2011).

[20] M. Nakano, P. Selles, P. Lablanquie, Y. Hikosaka, F. Penent, E. Shigemasa, K. Ito and S. Carniato, Phys. Rev. Lett., **111**, 123001 (2013).

[21] S. Carniato, P. Selles, P. Lablanquie, J. Palaudoux, L. Andric, M. Nakano, Y. Hikosaka, K. Ito, T. Marchenko, O. Travnikova *et al.*, Phys. Rev. A, **94**, 013416 (2016).

[22] R. Püttner, G. Goldsztejn, D. Céolin, J.-P. Rueff, T. Moreno, R. K. Kushawaha, T. Marchenko, R. Guillemin, L. Journel, D. W. Lindle *et al.*, Phys. Rev. Lett., **114**, 093001 (2015).

[23] G. Goldsztejn, T. Marchenko, R. Püttner, L. Journel, R. Guillemin, S. Carniato, P. Selles, O. Travnikova, D. Céolin, A. F. Lago *et al.*, Phys. Rev. Lett. **117**, 133001 (2016)

[24] A. Rudenko, L. Inhester, K. Hanasaki, X. Li, S. J. Robatjazi, B. Erk, R. Boll, K. Toyota, Y. Hao, O. Vendrell *et al.*, Nature **546**, 129 (2017).

[25] M. M. Seibert, T. Ekeberg, F. R. N. C. Maia, M. Svenda, J. Andreasson, O. Jönsson, D. Odić, B. Iwan, A. Rocker, D. Westphal *et al.*, Nature **470**, 7881 (2011).

[26] S. Boutet, L. Lomb, G. J. Williams, T. R. M. Barends, A. Aquila, R. B. Doak, U. Weierstall, D. P. DePonte, J. Steinbrener, R. L. Shoeman *et al.*, Science **337**, 362364 (2012).

[27] M. Kavčič, M. Budnar, A. Muhleisen, F. Gasser, M. Žitnik, K. Bučar and R. Bohinc, Rev. Sci. Instrum. **83**, 033113 (2012)

[28] D. Céolin, J. M. Ablett, D. Prieur, T. Moreno, J.-P. Rueff, T. Marchenko, L. Journel, R. Guillemin, B. Pilette, T. Marin *et al.*, J. Electron Spectrosc. Relat. Phenom., **190**, 188 (2013).

[29] J.-P. Rueff, J. M. Ablett, D. Céolin, D. Prieur, T. Moreno, V. Balédent, B. Lassalle, J. E. Rault, M. Simon, and A. Shukla, J. Synchrotron Rad. **22**, 175179 (2015)

[30] See Supplemental Material at [URL will be inserted by publisher] for assignment of $L_3M_{4,5}M_{4,5}$ Auger lines in CH_3I at the I L_3 edge.

[31] E.Kukk, G.Snell, J.D.Bozek, W.-T.Cheng, and N.Berrah, Phys. Rev. A **63**, 062702 (2001).

[32] E. Kukk, K. Ueda, U. Hergenhahn, X.-J. Liu, G. Prümper, H. Yoshida, Y. Tamenori, C. Makochekanwa, T. Tanaka, M. Kitajima *et al.*, Phys. Rev. Lett. **95**, 133001 (2005).

[33] T. Åberg and B. Crasemann, Phys. Rev. A, in *X-ray Resonant Anomalous Scattering* (Elsevier, Amsterdam 1994).

[34] F. Gel'mukhanov and H. Ågren, Phys. Rev. A, **54**, 379 (1996).

[35] J. L. Campbell and T. Papp, At. Data Nucl. Data Tables **77**,1 (2001).

[36] M. Polasik, K. Slabkowska, J. Rzadkiewicz, K. Koziol, J. Starosta, E. Wiatrowska-Koziol, J.-Cl. Dousse, and J. Hoszowska, Phys. Rev. Lett., **107**, 073001 (2011)

[37] M. Žitnik, R. Püttner, G. Goldsztejn, K. Bučar, M. Kavčič, A.Mihelič, T. Marchenko, R. Guillemin, L. Journel, O. Travnikova et al., Phys. Rev. A **93**, 021401(R) (2016).

[38] M. Kivilompolo, A. Kivimki, M. Jurvansuu, H. Aksela, S. Aksela, and R.F. Fink, J. Phys. B **33**, L157 (2000)

[39] Z. W. Gortel, R. Teshima and D. Menzel, Phys. Rev. A, **60**, 2159 (1999).

[40] P. Jönsson, X. He , C. Froese Fischer, I. P. Grant, Comput. Phys. Commun. **177**, 597 (2007).

[41] H.-J. Werner, P. J. Knowles, G. Knizia, F. R. Manby, and M. Schtz, WIREs Comput. Mol. Sci. **2**, 242 (2012).

[42] T. H. Dunning, J. Chem. Phys. **90**, 1007 (1989).

[43] D. E. Woon and T. H. Dunning, J. Chem. Phys. **98**, 1358 (1993).

[44] M. Reiher and A. Wolf, J. Chem. Phys. **121**, 2037 (2004); **121**, 10945 (2004).

[45] A. Wolf, M. Reiher, and B. A. Hess, J. Chem. Phys. **117**, 9215 (2002).

[46] E. J. Heller, J. Chem. Phys., **62**, 1544 (1975).

[47] S.-Y. Lee and E. J. Heller, J. Chem. Phys., **71**, 4777 (1979).